UDC 539.4

# Effect of Pores on Mechanical Behavior. Application to the Composite Material

## A. Salih,[a] O. Fassi Fehri,[b] S. Charif d'Ouazzane,[c] and Z. Azari[d]

[a] Industrial Engineering Laboratory, Rabat Institute, Rabat, Maroc

[b] Laboratoire de Mécanique et Matériaux, Faculté des Sciences, Rabat, Maroc

[c] Laboratoire de Modélisation et Calcul en Mécanique, Rabat, Maroc

[d] Laboratoire de Fiabilité Mécanique, Université de Metz, Metz, France

УДК 539.4

# Влияние пор на механическое поведение. Случай композитного материала

## А. Салих[а], О. Фасси Фехри[б], С. Шариф д'Уаззан[в], З. Азари[г]

[а] Лаборатория промышленного строительства, Рабат, Марокко

[б] Лаборатория механики и материалов, Рабат, Марокко

[в] Лаборатория моделирования и расчетов в механике, Рабат, Марокко

[г] Лаборатория механической надежности, Метц, Франция

*Выполнены экспериментальное исследование и численное моделирование влияния микроскопических пор на поведение вязкого материала при деформировании с учетом истории нагружения. Объектом исследования служил композитный материал на основе полиэстерной резины с включениями из бисера. В процессе формовки указанных компонентов в материале образуются поры из-за вязкости резины. Для оценки эффекта пор использовали экспериментальную технологию испытаний на растяжение. В рамках микромеханического подхода получены основные уравнения пороупругопластичности. Проведено обобщение модели материала Гурсона на исследуемый композитный материал. Результаты расчетов сопоставлены с экспериментальными данными.*

**Introduction.** The mechanical behavior of multiphase materials is related not only to the properties of various components but also to the interfacial adhesion between those constituents.

Generally, conventional composite materials contain pores introduced either as by-products of the thermomechanical process or intentionally to control microstructural features. During deformation, the inclusions may be debonded from the matrix including the new pores. Consequently, those nucleating pores grow by the plastic deformation.

There is considerable interest in the development of experimental [1] and analytical [2] methods for the characterization of the pore nucleation and growth process.

The best known experimental technique is tensile dilatometry (recently reviewed by Meddad et al. [3]). In this method, the volume change in the material is measured during the mechanical loading. Meddad et al. [3], who work with bead-filled plastic, operate with a section of the tensile stress-strain curve and also report that when tensile data are plotted using the compliance versus strain presentation, the various stages of the stress-strain curve are easily distinguished.

Analytically, there are significant developments of pore nucleation and growth process; we list those developed by Gurson [4, 5] on the ductile solid material containing pores. Our work parallels that of Chu and Needleman [6], who analyzed numerically the effects of pore nucleation in the biaxially stretched sheets.

In this work, we present the extension of the famous Gurson model [4, 5] to the porous composite material. The introduction of the pore pressure and the current porosity to that model allows to describe the material behavior. Based on the Bridgman [7] approach, we have also developed a new model of the nucleation porosity.

The theory of isotropic poroelastopasticity is introduced in section 1. The Hooke's relations and micromechanical constitutive constants are briefly listed in order to facilitate the engineering applications. A detailed description of the poroelastic theory was introduced by Biot [8]. An extended review of the development of the isotropic theory can be found in Detournay and Cheng [9]. Considering the same formality of continuous media, Coussy [10] presented the mechanical behavior of porous media according to the micromechanical analysis.

In section 2, a brief description of the experimental method is given. Using the dilatometry theory, the terminology used and the technique for obtaining the experimental data are based on [11]. In glass bead-filled unsatured polyester (UP), the global behavior is nonlinear. This behavior is characterized by the stress and pore pressure methods. The interfacial debonding will be suggested by the current porosity. The porous material model that has been developed by Gurson and the applications of the Euler integration to that model are also given in section 3. A comparison of the numerical results with those obtained from the experimental study close this paper.

1. **Poroelastoplastic Constitutive Relations**. Let us consider a geometrical domain $\Omega$ constituted by a fluid phase (pores) and solid (matrix) one, having in its initial configuration, the voluminal fraction $\phi_0$ and $(1 - \phi_0)$, respectively. In the case of poroelastoplastic configuration, we make an elementary dump defined by $d\sigma$ increments; we, respectively, measure the reversible $(d\varepsilon^e, d\zeta^e)$ and irreversible $(d\varepsilon^p, d\zeta^p)$ increments of strain and the variation of fluid content, such that

$$d\varepsilon = d\varepsilon^e + d\varepsilon^p, \tag{1}$$

$$d\zeta = d\zeta^e + d\zeta^p, \tag{2}$$

where $d\varepsilon$ and $d\zeta$ are, respectively, a differential change in the total strain and the total variation of fluid content.

In the framework of the hypothesis of infinitesimal transformations and for the case of linear poroelasticity, the changes in the stress $\sigma$ and pore pressure $p$, which represents the internal forces in the material, are defined in the following relations:

$$\sigma_{ij} = C_{ijkl}^{\gamma} \varepsilon_{kl}^{e},\tag{3}$$

$$p = M(\zeta^{e} - \alpha \varepsilon_{kk}^{e}),\tag{4}$$

where $C_{ijkl}^{\gamma}$ is the modulus tensor

$$C_{ijkl}^{\gamma} = \left(K_{\gamma} - \frac{2}{3}G_{\gamma}\right)\delta_{ij}\delta_{kl} + 2G_{\gamma}\delta_{ik}\delta_{jl}.\tag{5}$$

The superscript $\gamma = u$ (resp. $\gamma = d$) denotes undrained (resp. drained) quantities. The undrained modulus tensor $C_{ijkl}^{u}$ satisfies the following relation:

$$C_{ijkl}^{u} = C_{ijkl}^{d} + \alpha^{2} M I_{ijkl},\tag{6}$$

where $I_{ijkl}$ is a fourth order identity tensor, $\alpha$ is the Biot's coefficient, and $M$ is a modulus associated with the combined fluid/solid compressibility.

$$\alpha = 1 - \frac{K_{d}}{K_{m}} \quad \text{and} \quad M = K_{m}\left[\left(1 - \frac{K_{d}}{K_{m}}\right) - \phi_{0}\left(1 - \frac{K_{m}}{K_{f}}\right)\right]^{-1}.\tag{7}$$

For the isotropic case, the flow function includes not only the first and the second invariants of the stress tensor but also pore pressure and state variables. This flow function is illustrated by the following formula:

$$F(\sigma_{H}, \sigma_{q}, p, H^{\alpha}) = 0,\tag{8}$$

where $H^{\alpha}$ ($\alpha = 1, 2, ..., n$) is a set of values. The function $F$ is defined whenever: $F < 0$ the response is purely poroelastic and $F = 0$ which is the consistence condition represent the current yield surface; $\sigma_{H}$ and $\sigma_{q}$, which are, respectively, the hydrostatic and the equivalent stress, are defined by the following relations:

$$\sigma_{H} = \frac{1}{3}\sigma I \quad \text{and} \quad \sigma_{q} = \sqrt{(3/2)ss},\tag{9}$$

where $I$ is the second order identity tensor and $s$ is the stress deviator.

With the above notation, the stress tensor can be written as

$$\sigma = \sigma_H I + \frac{2}{3}\sigma_q n. \tag{10}$$

The flow rules are written as

$$d\varepsilon^p = d\lambda\left(\frac{\partial g}{\partial\sigma_q}n + \frac{1}{3}\frac{\partial g}{\partial\sigma_H}I\right) \quad \text{and} \quad d\phi^p = d\lambda\left(\frac{\partial g}{\partial p}\right), \tag{11}$$

where $d\lambda$ is a positive potential scalar, $d\phi^p$ is a differential change in the plastic porosity, and $g = g(\sigma_H, \sigma_q, p, H^\alpha)$ is the yield potential. The first flow rule gives:

$$d\varepsilon^p = \frac{1}{3}d\varepsilon_H^p I + d\varepsilon_q^p n, \tag{12}$$

where

$$d\varepsilon_H^p = d\lambda\left(\frac{\partial g}{\partial\sigma_H}\right), \quad d\varepsilon_q^p = d\lambda\left(\frac{\partial g}{\partial\sigma_q}\right), \quad \text{and} \quad n = \frac{3}{2}\frac{s}{\sigma_q},$$

in which $d\varepsilon_q^p$ and $d\varepsilon_H^p$ are related by the '*dilatancy*' relation [10]

$$\frac{d\varepsilon_H^p}{d\varepsilon_q^p} = \delta, \tag{13}$$

where $\delta$ is the dilatational factor.

Using Eqs. (1) and (2), relations (3) and (4) can be incrementally rewritten as

$$\sigma_{t+dt} = C^\gamma \varepsilon_{t+dt}^\varepsilon = C^\gamma(\varepsilon_t^e + d\varepsilon^e) = \sigma^e - C^\gamma d\varepsilon^p. \tag{14}$$

$$p_{t+dt} = M[\zeta_t^e + d\zeta^e - \alpha(\varepsilon_{H_t}^e + d\varepsilon_H^e)] = p^e - M[d\zeta^p - \alpha d\varepsilon_H^p], \tag{15}$$

where

$$\sigma^e = C^\gamma(\varepsilon_t^e + d\varepsilon) \tag{16}$$

and

$$p^e = M[\zeta_t^e + d\zeta - \alpha(\varepsilon_{H_t}^e + d\varepsilon_H)], \tag{17}$$

where $t$ is the time at the start of the increment and $t + dt$ is the time at the end of the increment.

Using the Eqs. (5) and (12), we can rewrite the Eqs. (14) and (15) as

$$\sigma_{t+dt} = \sigma^e - K_\gamma d\varepsilon^p_H I - 2G_\gamma d\varepsilon^p_q n, \tag{18}$$

$$p_{t+dt} = p^e - M(d\zeta^p - \alpha d\varepsilon^p_H). \tag{19}$$

Finally, the poroplasticity model is achieved by describing the evolution of the state variables

$$dH^\alpha = \bar{h}^\alpha (d\varepsilon^p, d\phi^p, \sigma, p, H^\beta) \tag{20}$$

as far as the rate independent materials $\bar{h}^\alpha$ remain homogenous of degree one in $d\varepsilon^p$ and $d\phi^p$.

### 2. **Application**.

2.1. **Experimental**. *Material*. The material used in this study is constituted by the glass beads (type E) incorporated in the polyester (UP) resin. The average bead diameter is about 350 $\mu$m. During the moulding of these constituents, the pores remain in the composite because of the resin viscosity. The bead volume fraction $f$ and the initial porosity $f_0$ are obtained by the statistical method which is described in [11]. Using an Versamet-2 optical microscope, with magnification $\times 1600$, the material was visualized (see Fig. 1).
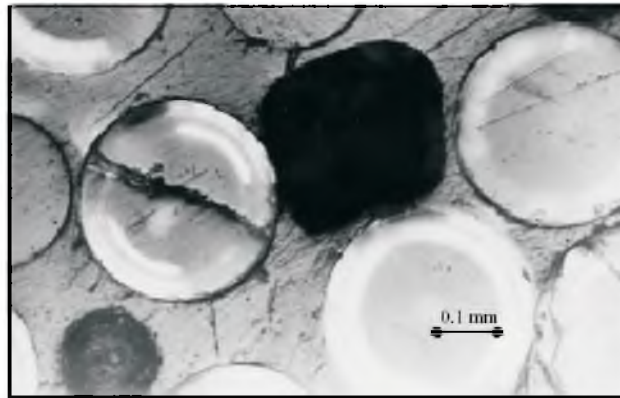


Fig. 1. Microscopic section of the material (resin in clear, beads in white, pores in black).

*Technical Test*. In order to determine the experimental data, we adopted the tensile test technique. This method is specified in [11]. The values of the mechanical characteristics are obtained in the undrained test, in which the variation of the fluid content is zero ($\zeta = 0$). A tensile test machine with the cross-head speed of 1 mm/mn was used. The strain data is collected by using two tensometers: axial tensometer and transverse tensometer (gauge length was 10 mm). The strains $\varepsilon$ and the stresses $\sigma$ were simultaneously recorded.

The stress $\sigma$ versus strain $\varepsilon$ curves for various initial porosity $\phi_0$ are shown in Fig. 2. It shows that the stress decreases with the porosity content. The behavior of these materials is nonlinear. The most plausible reason on this

nonlinearity is the debonding process. The effect of treatment of the glass beads interface appears negligible. It is difficult to separate the contribution of debonding and the behavior of the matrix because almost all the glass beads have became debonded from the matrix.
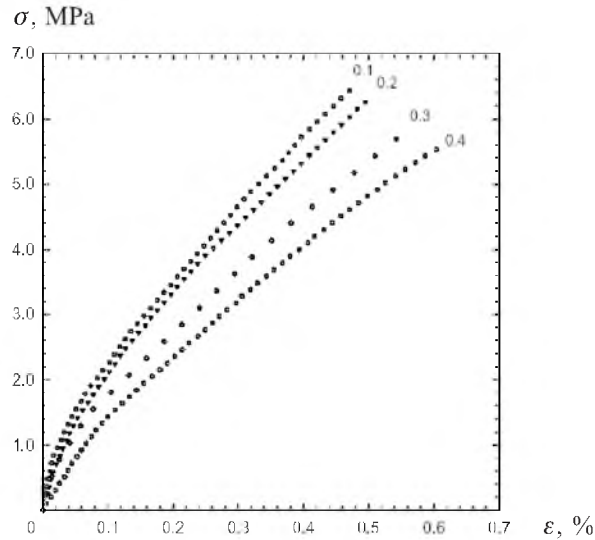


Fig. 2. Stress $\sigma$ vs nominal strain $\varepsilon$ for several values of $\phi_0$.

2.2. **Continuum Model of Porous Material**. In this section, the material model developed by Gurson [4, 5] for a porous ductile material is applied to the material studied. Based on an analysis of single spherical pore in a shell, including several simplified approximations (for example, the change of pore chap is neglected so that the yield function remains effectively isotropic), Gurson [4] proposed the following approximate form for the yield surface of periodically porous solid containing a volume fraction $\phi$ of pores:

$$F = \left(\frac{\sigma_q}{\sigma^m}\right)^2 + 2q_1\phi\cosh\left(\frac{3}{2}\frac{q_2\sigma_H}{\sigma^m}\right) - (1 + q_3\phi^2) = 0, \tag{21}$$

where $\sigma^m$ is the equivalent stress representing the actual microscopic stress state in the matrix material and $\phi$ is the current porosity. The parameters $q_1$, $q_2$, and $q_3$ (where $q_3 = q_1^2$) were introduced by Tvergaard [12] in an attempt to make the predictions of Gurson's equations. This assumption agrees with numerical studies of materials containing pores periodically distributed in the matrix. For $q_1 = q_2 = q_3 = 1$, the function (21) was obtained by Gurson for the spherical pores. The yield surface given by the equation (21) becomes that of von Mises when $\phi = 0$. Whenever the pore volume fraction is non-zero, there is an effect of the hydrostatic stress on the plastic flow.

The microscopic equivalent plastic strain $(\bar{\varepsilon}_q^p)$ is assumed to be governed by the equivalent plastic work

$$\sigma d\varepsilon^{p} = (1-\phi_0)\sigma^{m}d\bar{\varepsilon}_{q}^{p}$$ (22)

or, equivalently

$$d\bar{\varepsilon}_{q}^{p} = \frac{\sigma d\varepsilon^{p}}{(1-\phi_0)\sigma^{m}}.$$ (23)

The change in pore volume fraction during an increment of deformation is partly due to growth of the existing pores and partly due to nucleation of now pores by cracking or interfacial decohesion of inclusions or precipitate particles. Accordingly, we write

$$d\phi = d\phi_{G} + d\phi_{N}.$$ (24)

The growth of pores is related to the change of the total volume as

$$d\phi_{G} = (1-\phi_0)d\varepsilon_{H}^{p}.$$ (25)

*Suggestion of Chu and Needleman [6].* The second phase particles are the primary source of internal cavitations (pores). Pores initiate either by cracking of the inclusions or by decohesion of the inclusion matrix interface. Assuming that plastic strain controls nucleation process, as suggested by Chu and Needleman [6] we get

$$d\phi_{N} = Ad\bar{\varepsilon}_{q}^{p}.$$ (26)

Parameter $A$ depends in same complicated way on the distribution of the inclusions and the mean equivalent plastic strain for nucleation $\varepsilon_{N}$;

$$A = \frac{f_{N}}{s_{N}\sqrt{2\pi}}\exp\left(-\frac{1}{2}\left(\frac{\bar{\varepsilon}_{q}^{p} - \varepsilon_{N}}{s_{N}}\right)^{2}\right),$$ (27)

where $s_{N}$ is the standard deviation of the distribution and $f_{N}$ is determined so that the total volume fraction nucleated is consistent with the volume fraction of inclusions.

*New Model of the Nucleation Porosity.* The model of porous ductile material to be studied here is defined by a periodical arrangement of the spherical inclusions (beads) in the elastic-plastic media, as shown in Fig. 3. Referring to the microscopic scale, we also denote by $d\Omega_{0}^{m}$ and $d\Omega_{t}^{m}$ the initial and the current elementary domain of the matrix material and $d\Omega_{t}^{b}$ is the volume occupied at time $t$ by the nucleating inclusions initially located in $d\Omega_{0}^{b}$, so that $d\Omega_{0} = = d\Omega_{0}^{m} \cup d\Omega_{0}^{b}$ and $d\Omega_{t} = d\Omega_{t}^{m} \cup d\Omega_{t}^{b}$.

At time $t$ the total volume strain of the material is irreversible and is sum of the constituents which are related to:

(i) growth of the available pores;

(ii) decohesion of matrix-bead interface;

(iii) formation of new pores.

The second constituent is ignored in this study.

Here, we suppose that the pores grow as the spherical cavities once they nucleated. Based on an analysis of a elementary volume which contains a simple spherical inclusion in a matrix media, we consider the equivalent plastic strain in the material ($\varepsilon_q^p$) which controls the nucleation of new pores as such [7]

$$\varepsilon_q^p = 2 \ln\left(\frac{R_t}{R_0}\right),\tag{28}$$

where $R_0$ and $R_t$ are, respectively, the initial and the current radii of the inclusion. Equation (28) is validated in two cases:

1) we assume that the behavior of the matrix material is elastic. In this case the plastic strain is controlled by the pore volume strain;

2) the matrix is assumed to satisfy the incompressibility condition but, because of the existence of pores, the macroscopic response does not. This remark has been explicitly used by several authors (see for example [5] and [6]).
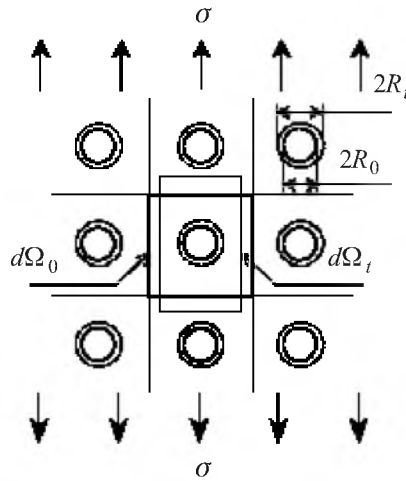


Fig. 3. Geometrical model of porous material.

Furthermore the material elementary volumes are defined as

$$d\Omega_0 = dX_1 dX_2 dX_3 \qquad \text{and} \qquad d\Omega_t = dx_1 dx_2 dx_3,\tag{29}$$

where $X_i$ and $x_i$ ($i = 1, 2, 3$) are the initial and the current positions so that $dx_i = dX_i + \delta dX_i$.

Let $P$ be the deformation gradient of the material so that $J = \det P$. It can be shown that

$$d\Omega_t = J d\Omega_0\tag{30}$$

and

$$J = 1 + \xi, \tag{31}$$

where $J$ is the Jacobian of the transformation and $\xi$ is the volume strain of the material. Using Eqs. (29), (30), and (31) the volume strain $\xi$ is expressed as

$$\xi = \left(1 + \frac{\delta dX_1}{dX_1}\right)\left(1 + \frac{\delta dX_2}{dX_2}\right)\left(1 + \frac{\delta dX_3}{dX_3}\right) - 1, \tag{32}$$

where $\varepsilon_L = \dfrac{\delta dX_1}{dX_1}$ and $\varepsilon_T = \dfrac{\delta dX_2}{dX_2} = \dfrac{\delta dX_3}{dX_3} = -\nu\varepsilon_L$ represent, respectively, the longitudinal and the transverse strains and $\nu$ is the Poison's ratio. In the plastic phase (or when the elastic phase is neglected) the volume strain is defined as

$$\xi = (1 + \varepsilon_L^p)(1 - \nu\varepsilon_L^p)^2 - 1. \tag{33}$$

This equation is equally valuated in the parfait plasticity case.

By using Eqs. (30) and (31), relationships (28) can be rewritten as

$$\varepsilon_q^p = \frac{2}{3}\ln\left(\frac{d\Omega_t^b}{d\Omega_0^b}\frac{d\Omega_t}{d\Omega_0}(\xi + 1)\right), \tag{34}$$

$$\varepsilon_q^p = \frac{2}{3}\ln\left(\frac{\phi_N}{f_N}(\xi + 1)\right), \tag{35}$$

where $\phi_N = \dfrac{d\Omega_t^b}{d\Omega_t}$ and $f_N = \dfrac{d\Omega_0^b}{d\Omega_0}$ are, respectively, the volume fractions of nucleation pores and of the inclusions that are susceptible to be cracked or nucleated.

Thus, the rate of the nucleated porosity $d\phi_N$ is obtained by the following formula

$$d\phi_N = \left[\frac{3}{2}\frac{f_N}{\xi + 1}\exp\left(\frac{3}{2}\frac{\varepsilon_H^p}{\delta}\right)\right]d\varepsilon_q^p = Sd\varepsilon_q^p, \tag{36}$$

where $\delta$, which is defined by the Eq. (13), is the dilatational factor of the material. To introduce it, let us consider the elementary experience that only the hydrostatic strain $\varepsilon_H$ and the distortion $\gamma_q = \dfrac{\varepsilon_q}{\sqrt{3}}$ are not null. If $\varepsilon_H^p$ and $\varepsilon_q^p$ correspond to the plastic contributions, the factor $\delta$ is defined by the relationship:

$$\delta = \frac{\varepsilon_H^p}{\varepsilon_q^p},$$

where, in the isotropic conditions, we get

$$\varepsilon_H^p = (1 - 2\nu)\varepsilon_L^p \qquad \text{and} \qquad \varepsilon_q^p = (1 + \nu)\varepsilon_L^p. \tag{37}$$

Finally, using the above remarks and Eq. (37), we find

$$\delta = \frac{1 - 2\nu}{1 + \nu}. \tag{38}$$

3. **Numerical Integration**. Using the equations given in Section 1, and enforcing the consistency condition $(dF = 0)$:

$$dF = \frac{\partial F}{\partial \sigma} d\sigma + \frac{\partial F}{\partial \sigma^m} d\sigma^m + \frac{\partial F}{\partial \phi} d\phi = 0. \tag{39}$$

By posing

$$\gamma = \frac{1}{2} q_1 q_2 \phi \sinh\left(\frac{1}{2} q_2 \omega\right), \tag{40}$$

$$\varphi = q_1 \cosh\left(\frac{1}{2} q_2 \omega\right) - q_3 \phi, \tag{41}$$

$$B = \frac{\omega(\omega + \gamma)}{1 - \phi_0}, \tag{42}$$

$$H = \frac{d\sigma^m}{d\bar{\varepsilon}_q^p} B^2 - \sigma^m A\varphi B - 3\sigma^m (1 - \phi_0)\gamma\varphi, \tag{43}$$

and

$$C = \frac{d\varepsilon}{d\varepsilon_q^p} = 1 + \frac{\gamma}{\omega} + \frac{H}{EB(1 - \phi_0)}, \tag{44}$$

where

$$\frac{d\bar{\varepsilon}_q^p}{d\varepsilon} = \frac{\omega + \gamma}{C(1 - \phi_0)}, \tag{45}$$

and after some algebraic manipulations, we find that the equations describing the poroelastoplastic problem can be written as

$$\frac{d\sigma}{d\varepsilon} = \frac{H}{CB(1-\phi_0)},$$ (46)

$$\frac{dp}{d\varepsilon} = \frac{3\alpha M\gamma}{C\omega},$$ (47)

$$\frac{d\phi}{d\varepsilon} = \frac{3\gamma}{C\omega}(1-\phi_0) + \frac{A(\omega+\gamma)}{C(1-\phi_0)},$$ (48)

where $\sigma$ and $\varepsilon$ are, respectively, the true macroscopic axial stress and logarithmic strain. The set of nonlinear equations (46), (47) and (48) is integrated using the Euler method with equal strain increments of $1/1000$ of the yield strain in order to ensure high accuracy. The results of this 'exact' solution are compared with those experimentally obtained.

From this comparison, let us consider the behavior of the composite material with an initial porosity at $\phi_0 = 0.2$. The uniaxial stress–strain curve of the matrix is represented in the following way:

$$\varepsilon^m = \begin{cases} \dfrac{\sigma^m}{E_m} & \text{for} \quad \sigma^m \le \sigma_Y^m, \\[2ex] \left(\dfrac{\sigma^m - \sigma_Y^m}{K_y}\right) & \text{for} \quad \sigma^m > \sigma_Y^m, \end{cases}$$ (49)

where $\varepsilon^m$ is the logarithmic strain, $\sigma^m$ is the true stress, $\sigma_Y^m$ is the uniaxial yield stress. The coefficients $K_y$ and $M_y$ are, respectively, the plastic strength and the hardening exponent. The elastic and plastic properties of the matrix are specified by $E_m/\sigma_Y^m = 4000$, $v_m = 0.4$, $K_y = 1100$ MPa, and $M_y = 1.33$, where $E_m$ is the Young modulus and $v_m$ is Poisson's ratio of the matrix material. The Tvergaard constants ($q_1$, $q_2$, and $q_3$) are equal to 1.

The plastic strain that controls the nucleation process is described by the volume fraction of nucleated or cracked beads $f_N = (1-\phi_0)f_0$, where $f_0$ is the bead volume fraction corresponding at $\phi_0 = 0$. The value of $f_0$ can be estimated in most cases to 0.52. Since the debonding process begins from the nominal strain at 0.03%, we have assigned this value to the $\varepsilon_N$, and the standard deviation is about $s_N = 0.06$.

The simulation test is assumed to be undrained. We suppose that the fluid enclosed in pores is a perfect gas. Consequently, for an isothermal transformation the fluid's bulk modulus is equal to the initial pore pressure $K_f = 0.1$ MPa.

The Biot's coefficients $\alpha$ and $M$ are calculated by the Eq. (7) in which the drained bulk modulus is obtained by the following formula:

$$K_d = K_u \left[ - \frac{\left(1 - \dfrac{K_m}{K_u}\right) - \phi_0 \left(1 - \dfrac{K_m}{K_f}\right)}{\left(1 - \dfrac{K_u}{K_m}\right) + \phi_0 \left(1 - \dfrac{K_m}{K_f}\right)} \right]. \tag{50}$$

In the studied range of axial strain (0–0.6%), the stress curve ($\sigma/\sigma_Y$), the rate of pore pressure ($\zeta p = \Delta p / p_0$) and the rate of the current porosity ($\zeta \phi = \Delta \phi / \phi_0$) are, respectively, plotted in Figs. 4, 5, and 6. These figures show that the numerical results (exact solutions) agree very well with those practically obtained.
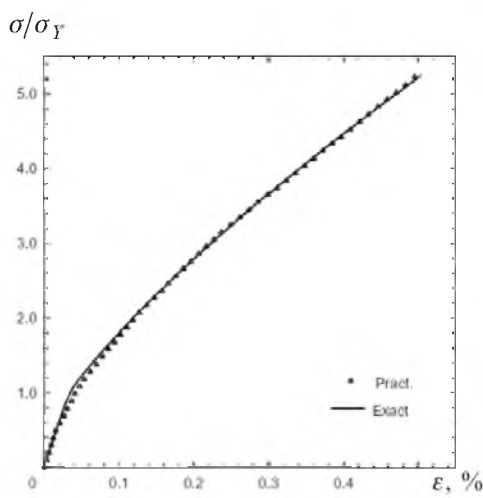


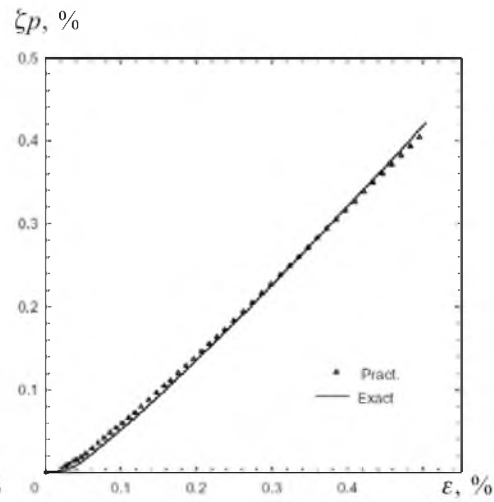Fig. 4. Uniaxial stress–strain curve.
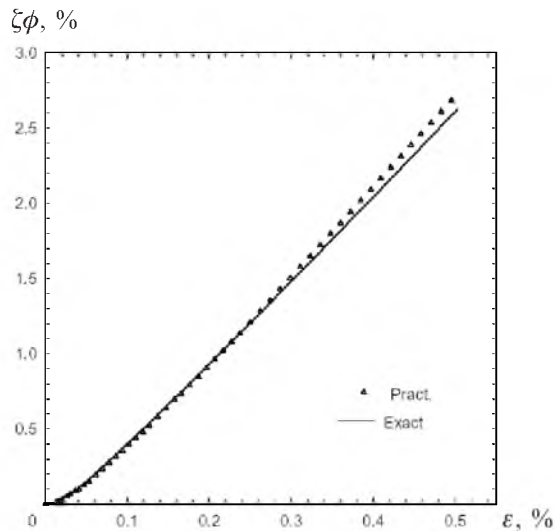
Fig. 5. Pressure rate $\zeta p$ vs nominal strain $\varepsilon$.



Fig. 6. Porosity rate $\zeta \phi$ vs nominal strain $\varepsilon$.

The behavior of porous composite material is described by the stress and the pore pressure. The interfacial debonding process is characterized by the current porosity $\phi$. The pores are assumed to grow as spherical cavities once they are nucleated. This is an appropriate idealization, in which nucleation takes place by debonding process.

The porosity influences significantly the stiffness and the characteristics of the material. Therefore, the behavior can be divided into three distinct stages:

I. Up to a deformation $\varepsilon = 0.03\%$, the behavior of this material is linear elastic with an initial modulus $E_0 = 5800$ MPa and initial Poisson's ratio $\nu_0 = 0.34$. The rate of the pore pressure ($\zeta p$) and the current porosity are zero. It is worth noting that between 0 and 0.03%, the plastic strain is zero. The 'loading–unloading' test illustrated this phenomena.

II. In the range of 0.03% and 0.12% the curves $\sigma(\varepsilon)$, $\zeta p(\varepsilon)$, and $\zeta\phi(\varepsilon)$ are nonlinear. This stage corresponds to the progressive debonding of the beads from the matrix. The value of the nucleation porosity $\phi_N$ is higher than that of the growing porosity $\phi_G$. When the porosity is not initially the case, the microbeads can sometimes be nucleated during straining in the second phase. The yield stress $\sigma_Y$, at which the debonding process is initiated, decreases with the increasing pores concentration.

III. At $\varepsilon = 0.12\%$, the $\sigma(\varepsilon)$ curve starts to deviate from nonlinearity to linearity. The porosity increases exponentially. After the glass beads are debonded from the matrix, it creates pores which grow by plastic deformation. This deformation of the pores created an additional porosity. In this stage, the behavior of porous composite material is similar to that of porous resin.
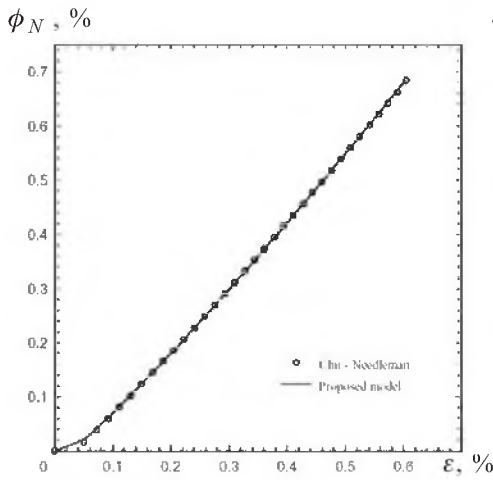


Fig. 7. Nucleation porosity $\phi_N$ vs strain $\varepsilon$ for Chu–Needleman's and proposed models.
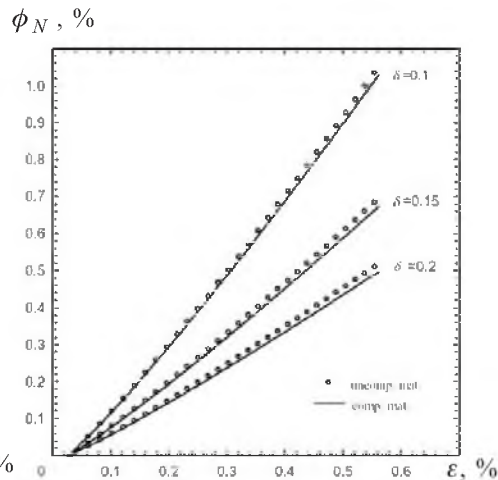
Fig. 8. Proposed model of $\phi_N$ for compressible and uncompressible material.

Having found the expression (36) for the new nucleation porosity model, the critical point of cracked beads into a shear band is pronounced in the behavior. This point is located at the nominal strain 0.03%. Figure 7 shows that the comparison, between the results of this model and those obtained by Chu and Needleman is conformed. This comparison between Chu and Needleman's

parameters at $\phi_0 = 0.2$, $\varepsilon_N = 0.03\%$, and $s_N = 0.06$ and the new model's coefficients $f_N = 0.416$. The parameters $\xi$ and $\delta$ are, respectively, obtained by the Eqs. (32) and (38). For the Poisson's ratio $0.3 \leq \nu \leq 0.4$ the dilatational factor is defined between $0.3 \leq \nu \leq 0.15$.

In view of this, the transformations related to the integration of Eqs. (39)–(48) yield to the formula that predicts a monotonous increase in $\phi_N$ with increasing strain, while the Chu–Needleman relation asserts that this value is not monotonic and even change rater at $\bar{\varepsilon}^p > \varepsilon_N$, but because the value taken in this study is very small, this phenomena no longer appears.

The effects of the volume strain of the matrix and the dilatational factor are illustrated in Fig. 8, which shows that the volume strain appears to be negligible. Therefore the study is similar to compressible or incompressible material, but the effect of the dilatational factor is significant.

**Conclusions**. In many situations, pores remain in the composite material during its moulding because of the viscosity of the resin. The pores modify not only the mechanism of load transfer between the matrix and the inclusions, but also the macroscopic characteristic. These pores are the origin of the stress concentration.

The problem analyzed in this study is the influence of the pores on the mechanical behavior.

On one hand, the poroelastoplastic formulation is developed in the isotropic case, according to the micromechanical consideration. The Gurson's material, in which we have introduced the new porosity model, is extended to the porous composite material. The application of the Euler integration method to the Gurson's model is discussed.

On the other hand, we have studied experimentally a material constituted from the microbeads of glass (E) which are incorporated in a polyester resin (UP).

From this study we deduce that the pores influence not only the characteristics of the material, but is also the nonlinearity of the behavior that has three distinct stages:

1). Linear poroelastic stage, where Young's modulus and Poisson's ratio are constant. In this stage, the current porosity and the pore pressure are neglected.

2). Debonding stage, in which the behavior deviates from linearity to nonlinearity. The debonding process is describing by the new model of the nucleation porosity. In this stage, the porosity increases exponentially.

3). Growing stage, in which the slope of the behavior decreases with the pores content. In this stage, that follows the complete debonding, the load of the bearing section is reduced by the area occupied by the glass beads.

We have also found that in the proposed model the effect of the incompressibility of the material appears to be negligible, but the dilatational factor influences significantly the nucleation porosity. This model consists in the replacement of the Chu–Needleman relation by a new one, which is more easy-to-use and more adapted to the micromechanics of this phenomena. However, the refinements proposed here cover mostly the expansion of an isolated spherical pore under uniaxial tensile loading conditions of a porous structure.

**Р е з ю м е**

Виконано експериментальні дослідження і числове моделювання впливу мікроскопічних пор на поведінку в'язкого матеріалу при деформуванні з урахуванням історії навантаження. Об'єктом дослідження служив композитний матеріал на основі поліестерної гуми з вкрапленнями з бісеру. У процесі формовки указаних компонентів у матеріалі з'являються пори внаслідок в'язкості гуми. Для оцінки ефекту пор використовували експериментальну технологію випробувань на розтяг. У рамках мікромеханічного підходу отримано основні рівняння поропружнопластичності. Проведено узагальнення моделі матеріалу Гурсона на композитний матеріал, що досліджується. Розрахункові результати зіставляються з експериментальними.

1. J. M. Jalinier, J. L. Salsmann, and B. Baudelet, "Strain hardening and damage," in: *Mechanical Behavior of Materials*, University of Cambridge (1979).

2. A. Needleman, and N. Triantafyllidis, "Void growth and local necking in biaxially stretched sheets," *J. Eng. Math. Tech.*, **100**, 164 (1978).

3. A. Meddad, S. Fellah, M. Pinard, and B. Fisa, "Filler-matrix debonding monitored by tensile test," *CRSP*, 1-5, E. Poly. de Montreal (1994).

4. A. L. Gurson, *Plastic Flow and Fracture Behavior of Ductile Materials Incorporating Void Nucleation, Growth, and Interaction*, Ph.D. Thesis, Brown University (1975).

5. A. L. Gurson, "Continuum theory of ductile rupture by void nucleation and growth: Part I. Yield criteria and flow rules for porous ductile materials," *J. Eng. Math. Tech.*, **99**, 2–15 (1977).

6. C. C. Chu and A. Needleman, "Void nucleation effects in biaxially stretched sheets," *J. Eng. Math. Tech.*, **102**, 249–256 (1980).

7. P. W. Bridgeman, *Studies in Large Plastic Flow and Fracture*, University Cambridge, Massachusetts, (1964).

8. M. A. Biot, "General theory of three-dimensional consolidation," *J. Appl. Phys.*, **12**, 155–164 (1941).

9. A. H. D. Cheng, "Material coefficients of anisotropic poroelasticity," *Int. J Rock. Mech. Min. Sci.*, **34**, 199–205 (1997).

10. O. Caussy, "Mécanique des milieux poreux," Technip, Paris (1991), pp. 89–217.

11. "Plastiques renforcés au verre textile," in: *France Association of Normalisation*, 2nd ed., AFNOR (1982), pp. 338–351, 396–399.

12. V. Tvergaard, "Influence of voids on shear band instabilities under plane strain," *Int. J. Fract.*, **17**, 389–407 (1981).